Transactions of the **13th International Conference on Structural Mechanics in Reactor Technology** (SMiRT 13), Escola de Engenharia - Universidade Federal do Rio Grande do Sul, Porto Alegre, Brazil, August 13-18, 1995

PWR pressure vessel stress analysis with axisymmetric model and harmonic loading

Albuquerque, L.B.[1], Assis, G.M.V.[1], Miranda, C.A.J.[2], Cruz, J.R.B.[2]
1) COPESP - Coordenadoria para Projetos Especiais, São Paulo, SP, Brazil
2) CNEN/SP-IPEN - Comissão Nacional de Energia Nuclear, São Paulo, SP, Brazil

ABSTRACT. The stress analysis of a PWR pressure vessel under postulated concentrated loads is presented. The vessel was modeled with four noded axisymmetric solid shell elements with harmonic load capacity. The vessel torispherical head was included in the model, but its evaluation is not within the scope of this work. The loads considered in the analyses were: internal pressure, dead weight, bolt-tightening, seismic load, and some postulated concentrated loads, that were modeled by Fourier Series. From the axisymmetric model, the stress results were taken at appropriate circumferencial positions and, for each position, the stresses were linearized at critical sections along the vessel for verification according to the ASME Code.

1 INTRODUCTION

This paper presents a nuclear reactor pressure vessel stress analysis. The ASME Section III, Subsection NB (ASME 1989) is adopted for the stress verification. The vessel was considered to be an axisymmetric structure. However, some postulated non-axisymmetric loads also act on the vessel. With the use of the ANSYS program (De Salvo & Gorman 1992), a finite element axisymmetric model was developed. The model was built with a finite element having harmonic loading capability. The non-axisymmetric loads were represented by Fourier series. Some critical sections in the vessel were chosen for the stress verifications. In such sections, the stresses were categorized and linearized before proceeding to the stress verifications. The recommendations of the ASME Code (1969) and of Hechmer & Hollinger (1991) were followed closely. In order to draw some conclusions about stress linearization, the membrane + bending stresses (Pl + Pb) are obtained and compared, in two appropriate sections, using three different methods.

2 FINITE ELEMENT MODEL DESCRIPTION

The analysed pressure vessel is sketched in figure 1. Harmonic shell elements with 4 nodes and 3 degrees of freedom (dof) per node were used to model the vessel and its support skirt. Beam elements with 2 nodes and 3 dof per node were employed to represent the flanged connection bolts. The nodes at the bottom of the skirt had all the dof restrained. The nodes in the axis of symmetry had its applied boundary conditions varying depending

on the symmetry or not of the acting load. To model the contact between the flanges, a previous axisymmetric analysis, in which only the axisymmetric loads (dead weight, internal pressure and bolt-tightening forces) were considered. In this analysis, gap elements with 2 nodes and 2 dof per node were used to represent the interface between flanges. The results pointed out the closed gap elements and hence a "contact area" between the flanges could be estimated. Therefore, when the non-axisymmetric (horizontal) loads were applied, the flanges were coupled by the nodes in the appraised "contact area".

3. LOADS

Besides the usual design loads - such as dead weight, internal pressure, bolt-tightening and vertical earthquake loads - also the effects of an postulated impulsive horizontal dynamic load were considered. These effects were represented through an overpressure due to the water mass acceleration and some extra concentrated loads. These postulated loads, classified as Level C condition, together with the horizontal seismic ones, are non-axisymmetric and were, consequently, developed by Fourier series. Figure 1 shows the positions where these horizontal concentrated loads are applied:
R1 - horizontal reactions from the vessel internals over the vessel guides (lower vessel region); R2 - horizontal reactions from the vessel internals over the inferior vessel flange, and R3 - reactions (resultants from forces and moments) considering the structures supported by the vessel head, e.g., the guides of the control rods.

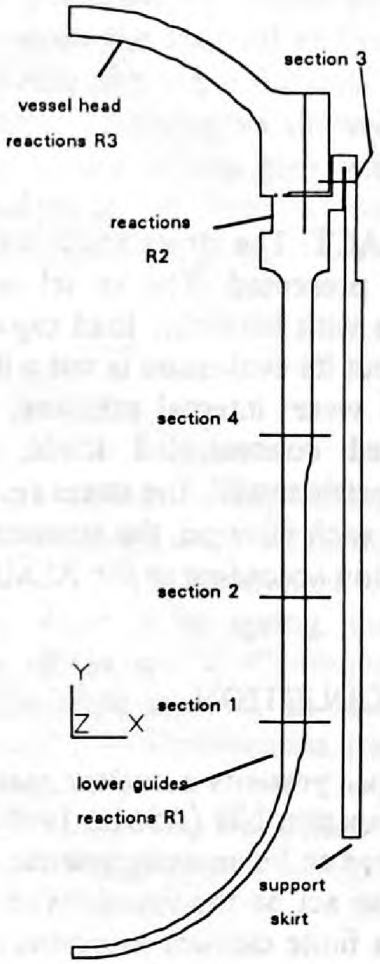

Figure 1 - Vessel Model

3.1 *Fourier Series (Reactions R1, R2 and R3).*

Reaction R1: It represents discrete loads acting on seven guides as shown in figure 2. To reduce the number of terms in the Fourier series, the discrete loads are approximated by a uniform load distribution, see eq. (1). Using the ANSYS program, the function $f1(\theta)$ was approximated by a Fourier series with five cosine terms.

Reaction R2: This load is concentrated in two opposite points at the inferior flange, as shown in Figure 3. To reduce the number of terms in the corresponding Fourier series this load was also approximated by a uniform load distribution R2 in equation (2). The function $f2(\theta)$ was developed by a Fourier series employing 32 sine terms.

Reaction R3: This loading is composed by horizontal forces and concentrated moments going at some points: one force and one moment for each control rod guide, instrumentation probes and detectors. For these structures, five groups with almost equal

radial position r were formed and the equivalent loads, for each group, were calculated. In all the groups the loading was a sum of a horizontal global force (defined by two components Fx cosθ + Fz sinθ; where Fx = -Fz) and a moment M reproduced by a Fy force distribution with a cosine development (M = Fy cosθ; were Fy = 2M/r). Therefore, these loads were developed by a Fourier series employing only one sine term and only one cosine term.

$$R1 \cong \int_0^{2\pi} f_1 \cos\theta \, d\theta \quad \text{where} \quad f_1(\theta) = \begin{cases} A\cos^2(4\theta/3) & 0 \le \theta \le 3\pi/8 \\ A\cos^2(4\theta/3 - 120) & 13\pi/8 \le \theta \le 2\pi \\ 0 & 3\pi/8 < \theta < 13\pi/8 \end{cases} \quad (1)$$

$$R2 \cong \int_0^{2\pi} f_2 \, d\theta \quad \text{where} \quad f_2(\theta) = \begin{cases} 0, \quad 0 \le \theta \le 17\pi/36;\ 19\pi/36 \le \theta \le 53\pi/36;\ \theta > 55\pi/36 \\ -B\cos^2(18\theta - 9\pi) & 7\pi/36 \le \theta \le 19\pi/36 \\ B\cos^2(18\theta - 9\pi) & 53\pi/36 < \theta < 55\pi/36 \end{cases} \quad (2)$$

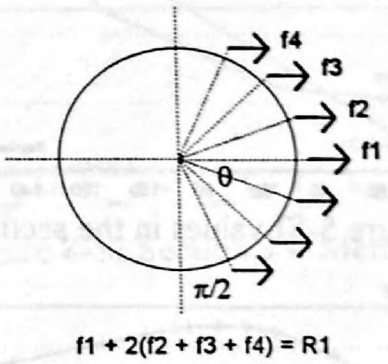

Figure 2 - R1 load in the lower guides

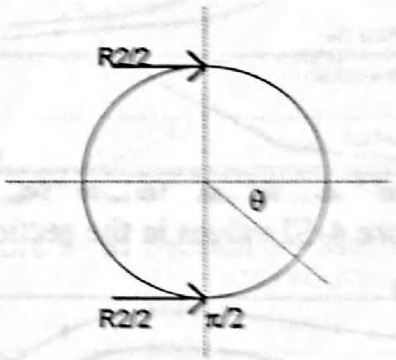

Figure 3 - R2 Load in the lower flange

Each coefficient of each series was input in the model as one load step. The order n of one generic term in the series, i.e., the number of waves associated with the Fourier term, was input as the MODE parameter (De Salvo & Gorman 1992). The boundary conditions, for those nodes on the axis of symmetry, were defined accordingly to the associated MODE parameter.

4 RESULTS: STRESS CLASSIFICATION and LINEARIZATION

In Figure 1, four critical vessel sections were selected for stress evaluations. For each section, the stresses were evaluated along 20 circumferential positions. For a section within $\sqrt{rt}$ from a geometric discontinuity (r and t are, respectively, the mean radius and the thickness of the vessel wall at that section), the membrane stress was classified as Pl. Away from any geometric discontinuity, the membrane stress was taken as Pm. The bending stresses were always classified as Pb, no matter whether the section is near or far from any discontinuity. In this work, three methods were adopted to linearize the stresses, named Methods I, II and III. Such methods differ on the way the stress components are treated to obtain the stress intensities. The results for the three methods will be compared for the sections numbers 3 and 4.

Method I - According to the discussions performed by Hechmer & Hollinger (1991), the stress linearization was made for all six components (three direct stresses and three shear stresses). The Stress Intensities (SI) values, in the four sections, along with the circumferential position are shown in Figures 4 to 7. In this case, the neutral surface is considered to be coincident with the center surface.

Method II - Linearization of the three direct stresses. The shearing stresses are considered to have a parabolic distribution and a zero value at the ends of the cross sections. This means that no bending contribution from the shearing stresses is acknowledged.

Method III - Linearization of two normal stresses (meridional stress, SY and hoop stress, SZ) and consideration of the membrane contribution for the through-tickness normal stress and shear components.

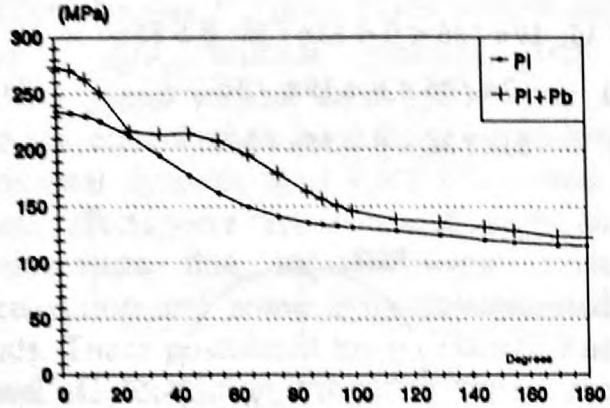

Figure 4-SI values in the section 1

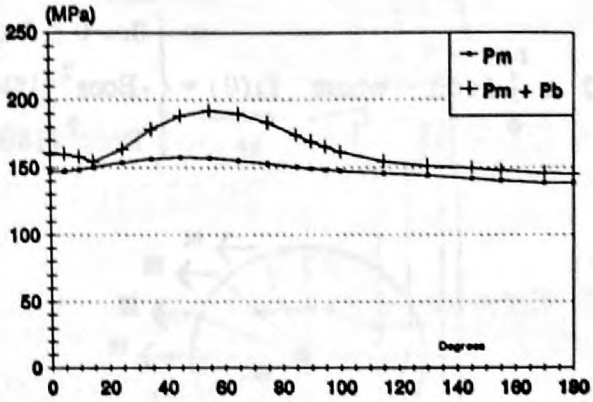

Figure 5-SI values in the section 2

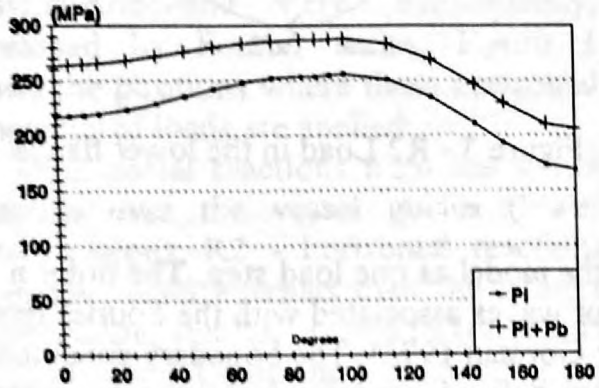

Figure 6-SI values in the section 3

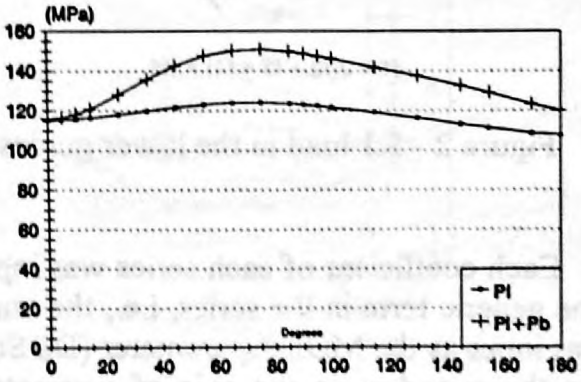

Figure 7-SI values in the section 4

General Remarks.

a) The effects due to the non-axisymmetric concentrated loads in section 2 may be neglected and, according to the ASME Code (1969), the membrane stress Pm can be obtained by equilibrium through the equation: $Pm = S_\theta + p$, where the hoop stress is $S_\theta = pr_1/t$, p is the internal pressure in the vessel, r_1 is the cylinder internal radius and t its thickness. Therefore, $Pm = p(r_1/t + 1) = 148.9$ MPa. This result agrees with Pm distribution shown in Figure 5. In that Figure, Pm curve has a slight oscillation around the obtained medium value 148.4 MPa.

b) The linearized stresses (Pl and Pl + Pb) were calculated in section 3 (located at 100^o in the circumferencial direction) and in section 4 (at 55^o). The linearized stresses were acquired from the FE model by the application of the three methods described before. The obtained values of Pl and Pl + Pb are reported in Table 1.

Table 1 - Sections 3 and 4 - Results at 100° and 55°

section	method	Figure	Pl	Pl+Pb
3 (at 100°)	I	8	255.9	287.7
	II	9	255.7	255.7
	III	10	255.7	255.5
4 (at 55°)	I	11	123.2	147.6
	II	12	123.	142.1
	III	13	123.1	138.9

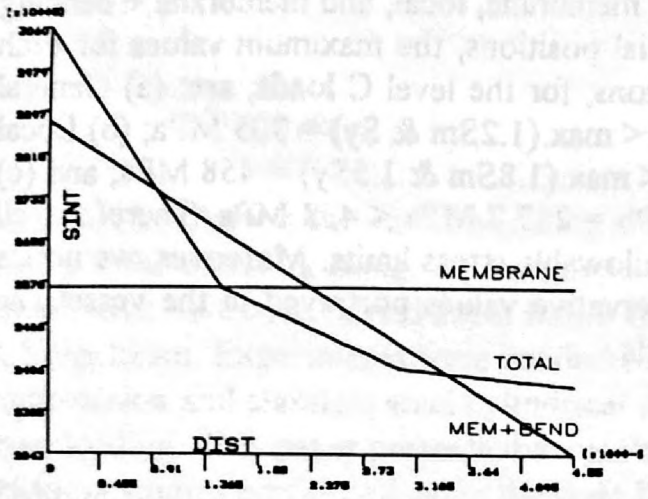

Figure 8-SI Section 3 - Method I

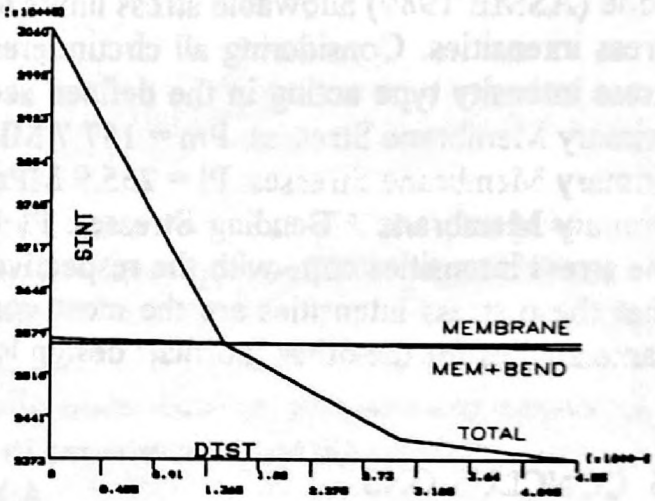

Figure 9- SI Section 3 - Method II

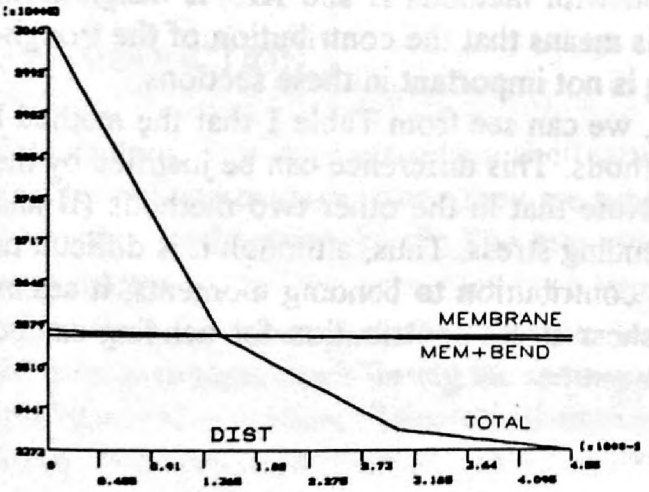

Figure 10 - SI Section 3 - Method III

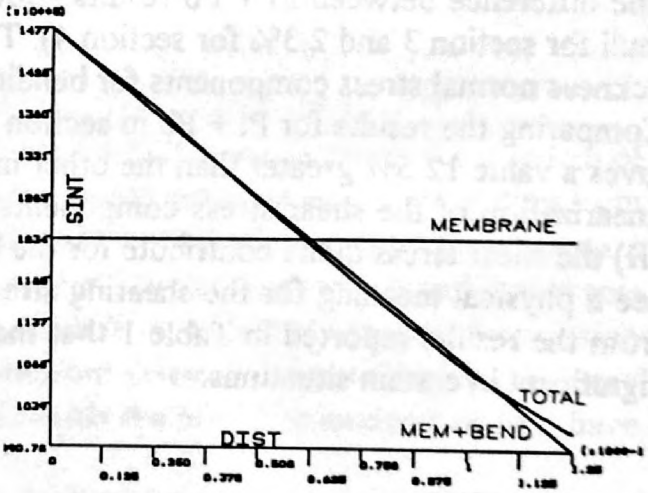

Figure 11-Section 4 - Method I

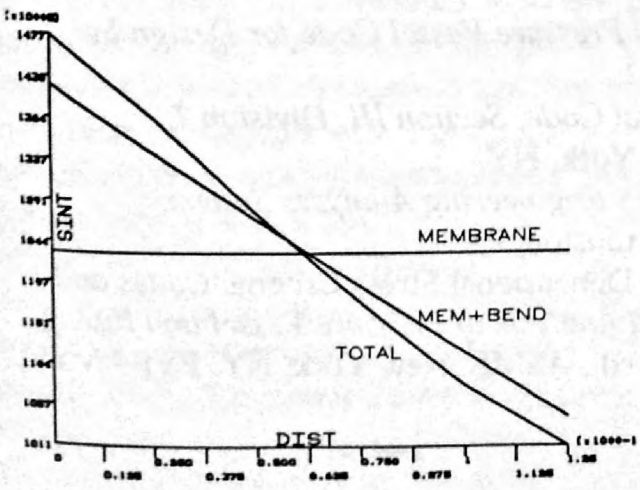

Figure 12-Section 4 - Method II

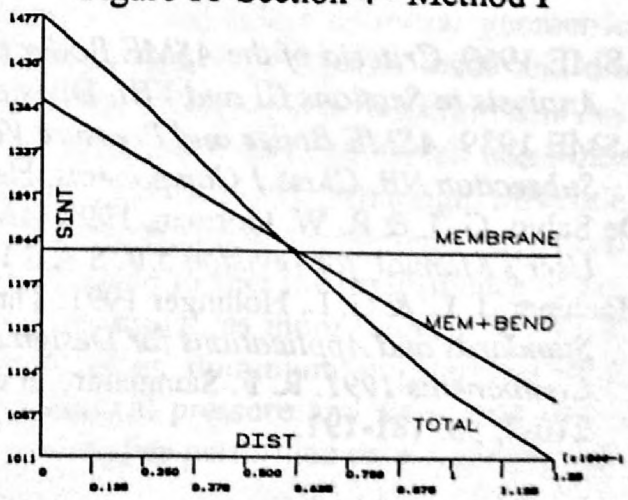

Figure 13-Section 4 - Method III

c) The distance between the neutral axis of the axisymmetric section to the center surface is, according to the ANSYS manual (De Salvo & Gorman 1992), $x_f = t^2/(12*Rc)$, where Rc and t are, respectively, the mean radius and section thickness. In method I, it has been assumed that there is a coincidence between the neutral surface and the center surface. The error due to this assumption was considered negligible since for section 3, $x_f = 0.148$ mm (Rc = 1.638 m, t = 0.125 m) and, for the section 4, $x_f = 0.131$ mm (Rc = 0.9925 m, t = 0.125 m).

Stress Verification. The stress verification is performed taking into account the respective Code (ASME 1989) allowable stress limits for membrane, local, and membrane + bending stress intensities. Considering all circumferencial positions, the maximum values for each stress intensity type acting in the defined sections, for the level C loads, are: (a) General Primary Membrane Stresses: Pm = 157.7 MPa < max.(1.2Sm & Sy) = 305 MPa; (b) Local Primary Membrane Stresses: Pl = 255.9 MPa < max.(1.8Sm & 1.5Sy) = 458 MPa; and (c) Primary Membrane + Bending Stresses: Pl + Pb = 287.7 MPa < 458 MPa. Therefore, all the stress intensities cope with the respective allowable stress limits. Moreover, we notice that these stress intensities are the most conservative values portrayed in the vessel.The same applies for the other "normal" design loads.

5. CONCLUSIONS

The difference between Pl + Pb results - found with methods II and III - is insignificant (null for section 3 and 2.3% for section 4). This means that the contribution of the trough-tickness normal stress components for bending is not important in these sections.
Comparing the results for Pl + Pb in section 3, we can see from Table 1 that the method I gives a value 12.5% greater than the other methods. This difference can be justified by the linearization of the shear stress components. Note that in the other two methods (II and III) the shear stress didn't contribute for the bending stress. Thus, although it is difficult to see a physical meaning for the shearing stress contribution to bending moments, it seams from the results reported in Table 1 that the shear stress contribution for bending can be significant in certain situations.

REFERENCES

ASME 1969. *Criteria of the ASME Boiler and Pressure Vessel Code for Design by Analysis in Sections III and VIII, Division 2.*

ASME 1989. *ASME Boiler and Pressure Vessel Code, Section III, Division 1, Subsection NB, Class 1 Components.* New York, NY.

De Salvo, G. J. & R. W. Gorman, 1992. *ANSYS Engineering Analyses System, User's Manual, for revision 5.0.* S.A.S.I., Houston, PA.

Hechmer, J. L. & G. L. Hollinger 1991. Three Dimensional Stress Criteria. *Codes and Standards and Applications for Design and Analysis of Pressure Vessel and Piping Components 1991.* R. F. Sammataro et al., ed., ASME. New York, NY. PVP - Vol. 210-2, pp. 181-191.